



This is a repository copy of *Fast-track adaptive laboratory evolution of Cupriavidus necator H16 with divalent metal cations*.

White Rose Research Online URL for this paper:

<https://eprints.whiterose.ac.uk/214813/>

Version: Published Version

Article:

Sitompul, S.N., Diaz Garcia, L.A., Price, J. et al. (2 more authors) (2024) Fast-track adaptive laboratory evolution of *Cupriavidus necator* H16 with divalent metal cations. *Biotechnology Journal*, 19 (7). 2300577. ISSN 1860-6768

<https://doi.org/10.1002/biot.202300577>

Reuse

This article is distributed under the terms of the Creative Commons Attribution (CC BY) licence. This licence allows you to distribute, remix, tweak, and build upon the work, even commercially, as long as you credit the authors for the original work. More information and the full terms of the licence here:

<https://creativecommons.org/licenses/>

Takedown

If you consider content in White Rose Research Online to be in breach of UK law, please notify us by emailing eprints@whiterose.ac.uk including the URL of the record and the reason for the withdrawal request.



eprints@whiterose.ac.uk
<https://eprints.whiterose.ac.uk/>

BIOTECH METHOD

Fast-track adaptive laboratory evolution of *Cupriavidus necator* H16 with divalent metal cations

Sepwin Nosten Sitompul¹ | Laura Andrea Diaz Garcia¹ | Joseph Price² |
Kang Lan Tee^{1,2}  | Tuck Seng Wong^{1,2,3,4} 

¹Department of Chemical & Biological Engineering, University of Sheffield, Sheffield, UK

²Evolutor Ltd, The Innovation Centre, Sheffield, UK

³National Center for Genetic Engineering and Biotechnology (BIOTEC), National Science & Technology Development Agency (NSTDA), Khlong Luang, Pathum Thani, Thailand

⁴School of Pharmacy, Bandung Institute of Technology, Bandung, West Java, Indonesia

Correspondence

Kang Lan Tee and Tuck Seng Wong,
Department of Chemical & Biological Engineering, University of Sheffield, Sir Robert Hadfield Building, Sheffield S1 3JD, UK.
Email: k.tee@sheffield.ac.uk and t.wong@sheffield.ac.uk

Funding information

National Research Council of Thailand, Grant/Award Number: P2250317/3; Engineering and Physical Sciences Research Council, Grant/Award Number: EP/X025853/1; Royal Academy of Engineering, Grant/Award Number: LTSRF1819-15-21

Abstract

Microbial strain improvement through adaptive laboratory evolution (ALE) has been a key strategy in biotechnology for enhancing desired phenotypic traits. In this Biotech Method paper, we present an accelerated ALE (aALE) workflow and its successful implementation in evolving *Cupriavidus necator* H16 for enhanced tolerance toward elevated glycerol concentrations. The method involves the deliberate induction of genetic diversity through controlled exposure to divalent metal cations, enabling the rapid identification of improved variants. Through this approach, we observed the emergence of robust variants capable of growing in high glycerol concentration environments, demonstrating the efficacy of our aALE workflow. When cultivated in 10% v/v glycerol, the adapted variant Mn-C2-B11, selected through aALE, achieved a final OD₆₀₀ value of 56.0 and a dry cell weight of 15.2 g L⁻¹, compared to the wild type (WT) strain's final OD₆₀₀ of 39.1 and dry cell weight of 8.4 g L⁻¹. At an even higher glycerol concentration of 15% v/v, Mn-C2-B11 reached a final OD₆₀₀ of 48.9 and a dry cell weight of 12.7 g L⁻¹, in contrast to the WT strain's final OD₆₀₀ of 9.0 and dry cell weight of 3.1 g L⁻¹. Higher glycerol consumption by Mn-C2-B11 was also confirmed by high-performance liquid chromatography (HPLC) analysis. This adapted variant consumed 34.5 times more glycerol compared to the WT strain at 10% v/v glycerol. Our method offers several advantages over other reported ALE approaches, including its independence from genetically modified strains, specialized genetic tools, and potentially carcinogenic DNA-modifying agents. By utilizing divalent metal cations as mutagens, we offer a safer, more efficient, and cost-effective alternative for expansion of genetic diversity. With its ability to foster rapid microbial evolution, aALE serves as a valuable addition to the ALE toolbox, holding significant promise for the advancement of microbial strain engineering and bioprocess optimization.

KEYWORDS

adaptive laboratory evolution (ALE), *Cupriavidus necator* H16, divalent metal cations, glycerol utilization, *Ralstonia eutropha* H16

This is an open access article under the terms of the [Creative Commons Attribution](https://creativecommons.org/licenses/by/4.0/) License, which permits use, distribution and reproduction in any medium, provided the original work is properly cited.

© 2024 The Author(s). *Biotechnology Journal* published by Wiley-VCH GmbH.

1 | INTRODUCTION

Adaptive laboratory evolution (ALE) has evolved as an indispensable and robust technique, instrumental in enhancing a multitude of microbial properties vital for biomanufacturing.^[1–3] These properties span from optimizing carbon utilization and improving microbial growth to enhancing tolerance against inhibitors and more. ALE stands out for its straightforward technical implementation and its applicability to diverse microbial strains. As a top-down methodology, it circumvents the need for intricate knowledge about the metabolic network of the microbe in question, as well as specialized equipment or a sophisticated genetic toolkit. This approach not only expedites the acquisition of valuable biological data but also facilitates reverse engineering, thereby unraveling crucial insights into the intricate dynamics of the phenotype–genotype interplay.

ALE has demonstrated its effectiveness in enhancing the properties of *Cupriavidus necator* H16 (formerly known as *Ralstonia eutropha* H16), a betaproteobacterium renowned for its inherent ability to accumulate polyhydroxyalkanoate (PHA) up to 90% of its dry cell weight. PHA, a diverse range of thermoplastic polyesters, offers customizable material properties that can be fine-tuned through the manipulation of monomer composition and molecular weight. The applications of ALE on *C. necator* H16 are wide-ranging. Key examples include improving glycerol utilization,^[4] increasing halotolerance,^[5] improving growth on formate,^[6] and enhancing carbon monoxide tolerance.^[7]

Notwithstanding its simplicity, the ALE process can be time-consuming, involving serial or continuous cultivation under selective conditions. To expedite the evolutionary process, expanding genetic diversity becomes crucial, necessitating the creation of a larger and more complex pool of variants for subsequent selection. This is commonly achieved through the application of physical agents (e.g., UV radiation) and chemical agents (e.g., DNA alkylating agents like ethyl methanesulfonate). Although divalent metal ions, such as Mn^{2+} , are extensively employed in random mutagenesis for protein evolution,^[8,9] their application in ALE remains unexplored.

This Biotech Method paper seeks to introduce a novel, accelerated ALE workflow by incorporating divalent metal ions. Initially, the impact of three divalent metal ions (Co^{2+} , Mn^{2+} , and Zn^{2+}) on the microbial growth of *C. necator* H16 was examined. Subsequently, these divalent metal ions were utilized to create genetic diversity and expedite the ALE process, facilitating the rapid identification of *C. necator* H16 variants capable of withstanding high concentrations of glycerol. This method marks the first application of divalent metal ions in ALE, presenting a significant advancement in the field.

2 | MATERIAL AND METHODS

2.1 | Bacterial strain and cultivation conditions

C. necator H16 (DSM 428) was cultivated in mineral salts medium (MSM; pH 7.0) with 1% w/v sodium gluconate^[10] or nutrient broth (NB; 5 g L⁻¹ peptone, 1 g L⁻¹ beef extract, 2 g L⁻¹ yeast extract,

5 g L⁻¹ sodium chloride), supplemented with 10 $\mu\text{g mL}^{-1}$ of gentamicin, at 30°C.

2.2 | The effect of divalent metal cations on the microbial growth of *C. necator* H16

To examine the impact of divalent metal cations on microbial growth, *C. necator* H16 was cultivated in Chi.Bio.^[11] This process was carried out in a capped 30-mL clear borosilicate glass vial (Thermo Fisher Scientific, catalogue number 11593532), containing 15 mL of NB medium. The medium was supplemented with 10 $\mu\text{g mL}^{-1}$ of gentamicin and varying concentrations of $CoCl_2$ (0–20 μM), $MnCl_2$ (0–25 mM), or $ZnCl_2$ (0–5 mM). A fresh medium was inoculated with an overnight culture, targeting a starting OD_{600} of 0.2. The cultivation took place at a temperature of 30°C, with continuous stirring at a speed setting of 0.6 using a disc-shaped PTFE stir bar (Thermo Fisher Scientific, catalogue number 11878892). Optical density was measured at 650 nm at regular intervals during the experiment. Chi.Bio operates at a fixed wavelength of 650 nm. We also replicated the experiment with *Escherichia coli*, following the same protocol, albeit with a modification in the cultivation medium from NB supplemented with gentamicin to Luria–Bertani (LB) medium.

2.3 | Accelerated adaptive laboratory evolution (aALE) for high glycerol tolerance

The aALE process was conducted in accordance with the workflow presented in Figure 1. Each evolution cycle comprised two distinct stages: mutagenesis and selection. To initiate mutagenesis, *C. necator* H16 was cultured in a 50-mL Falcon tube, containing 5 mL of MSM with 1% w/v sodium gluconate. This medium was supplemented with 10 $\mu\text{g mL}^{-1}$ of gentamicin and either 10 μM $CoCl_2$, 15 mM $MnCl_2$, or 0.7 mM $ZnCl_2$, and allowed to incubate for 15 h at 30°C. Subsequently, cells were collected through centrifugation at maximum speed for 2 min at room temperature. The cell pellet underwent two washes with 1 mL of MSM without any carbon source and was then appropriately diluted using the same medium. Moving to the selection stage, *C. necator* H16 was cultivated in Chi.Bio, utilizing a glass vial that contained 15 mL of MSM supplemented with 10% v/v glycerol, and 10 $\mu\text{g mL}^{-1}$ of gentamicin. The medium was inoculated with the diluted cells obtained from the preceding mutagenesis step, targeting an initial OD_{600} of 0.2. Cultivation was sustained until an early stationary phase was achieved, thus signaling the commencement of a new evolution cycle.

2.4 | Adapted variants characterization in 96-well microplates and personal bioreactor RTS-1

The adapted variants were subjected to characterization, with cultivation conducted either in a 96-well microplate or a personal bioreactor

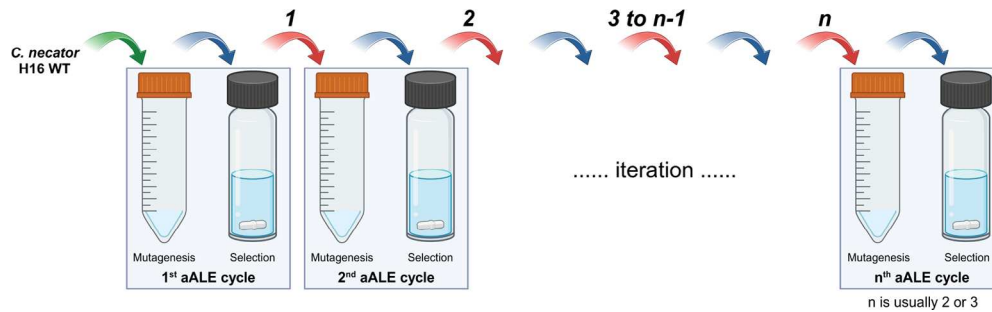


FIGURE 1 The workflow of accelerated adaptive laboratory evolution (aALE). Each aALE cycle involves the initial treatment of cells with 10 μM CoCl_2 , 15 mM MnCl_2 , or 0.7 mM ZnCl_2 during the mutagenesis stage, followed by cultivation in selective medium during the selection stage.

RTS-1 (Biosan). For the 96-well microplate cultivation, each well was filled with 150 μL of MSM, supplemented with 10 $\mu\text{g mL}^{-1}$ of gentamicin and 5% v/v glycerol. The microplate was placed on a Titramax 1000 shaker (Heidolph) operating at 30°C and 1050 rpm. Optical density was monitored at 595 nm using a Multiskan FC microplate photometer (Thermo Fisher Scientific). Alternatively, for cultivation in the personal bioreactor RTS-1, a 50-mL TPP TubeSpin bioreactor tube with a membrane filter was employed. The tube was loaded with 20 mL of MSM supplemented with 10 $\mu\text{g mL}^{-1}$ of gentamicin and 5%–15% v/v glycerol. Cultivation took place at 30°C, with the tube rotated at a speed of 2000 rpm, incorporating a 1 s^{-1} reverse spin. Optical density was tracked at 850 nm during the cultivation process. Personal bioreactor RTS-1 operates at a fixed wavelength of 850 nm. At the end of the cultivation, samples were collected for OD_{600} measurement, dry cell weight determination, and analysis of remaining glycerol in the spent medium using high-performance liquid chromatography (HPLC), as detailed below.

2.5 | Determination of glycerol utilization in *C. necator* H16 wild type and variants

Samples for analysis were first centrifuged at 21,000 $\times g$ for 5 min to separate the cells from the spent culture media. The supernatant was then diluted 5 \times for cells cultivated in 5% v/v glycerol, 10 \times for cells cultivated in 10% v/v glycerol, or 15 \times for cells cultivated in 15% v/v glycerol, using 0.005 N sulfuric acid. The diluted samples were clarified by filtration through a Corning Costar Spin-X centrifuge tube filter equipped with a cellulose acetate membrane (pore size: 0.22 μm) at 10,000 $\times g$ for 1 min to remove any remaining cell particles. Glycerol concentrations in the spent culture media were determined by HPLC using a Shimadzu Prominence-i LC-2030C Plus system. The HPLC was equipped with a Rezex ROA-Organic Acid column (300 \times 7.8 mm; Phenomenex) and a refractive index detector. Ten microliters of each sample were injected via an autosampler, and isocratic separation of glycerol was achieved at 60°C with 0.005 N sulfuric acid as the mobile phase, flowing at a rate of 0.6 mL min^{-1} . Glycerol concentrations were quantified using a standard curve generated from known concentrations of glycerol ($\geq 99\%$ purity; Sigma-Aldrich).

2.6 | Genomic DNA extraction

The extraction of genomic DNA was performed utilizing the GeneJET Genomic DNA Purification Kit (Thermo Fisher Scientific), following the manufacturer's instructions. The eluted DNA underwent an additional purification step through ethanol precipitation. In a 1.5-mL microcentrifuge tube, 20 μL of 3 M sodium acetate (pH 5.2) was mixed with 200 μL of column-eluted DNA. Following this, 200 μL of ice-cold absolute ethanol was added and the resulting mixture was briefly vortexed. Subsequently, the tube was stored at -20°C overnight. After the overnight incubation, the tube was subjected to centrifugation at maximum speed for 30 min at 4°C. The DNA pellet was then washed twice with ice-cold 75% ethanol, followed by an incubation at 37°C for 15–20 min to remove any residual ethanol. The DNA pellet was finally reconstituted in an appropriate volume of Elution Buffer (10 mM Tris-Cl, pH 9.0, 0.1 mM EDTA) provided in the GeneJET kit. The concentration and purity of the DNA sample were determined using the EzDrop 1000 microvolume spectrophotometer (Blue-Ray Biotech) and by electrophoresing 1 μg of DNA on a 1% w/v TAE gel.

2.7 | Genome sequencing

Microbial whole-genome sequencing was conducted by Novogene, employing the Illumina PE150 technology. Subsequently, the sequencing data was aligned with the reference sequences (GenBank CP039287.1, CP039288.1, and CP039289.1) through the use of BWA.^[12] Detection of single nucleotide variations (SNVs) and insertions/deletions (InDels) was executed using the GATK software.^[13] Variation annotation was performed utilizing the capabilities of ANNOVAR.^[14]

3 | RESULTS AND DISCUSSION

3.1 | Divalent metal cations affect the microbial growth of *C. necator* H16

Metal ions play a vital role in sustaining life, being essential for bacterial growth, with Zn^{2+} , Mn^{2+} , and Fe^{2+} cellular concentrations falling

within the range of 0.4–1 mM under favorable conditions.^[15] Metalloproteins depend on the presence of these ions to execute crucial functions, contributing to both the structure of proteins and the facilitation of catalytic activities.^[16] Instances of bacterial growth inhibition due to metal intoxication can result from the generation of harmful reactive oxygen species or the erroneous metalation of enzymes pivotal in critical metabolic pathways. Additionally, surpassing the threshold concentrations of these metal ions can disrupt the accuracy of DNA synthesis.^[17,18]

In this study, CoCl_2 , MnCl_2 , and ZnCl_2 were specifically chosen to evaluate their effects on microbial growth and their potential as chemical mutagens, intended to enhance the genetic diversity for ALE. CoCl_2 and MnCl_2 were categorized as class 1 compounds by Loeb and coworkers, leading to an elevation in error frequency and a decline in DNA synthesis in vitro.^[17] Conversely, ZnCl_2 was classified as a class 2 compound, which did not compromise fidelity but did result in reduced DNA synthesis. Notably, the mutagenic impact of 4 mM CoCl_2 and 10 mM MnCl_2 was observed to reduce fidelity by a minimum of 30%, while 0.4 mM ZnCl_2 had no significant effect on fidelity.^[17] Furthermore, MnCl_2 is frequently utilized in error-prone polymerase chain reaction (epPCR) for protein evolution, typically within the concentration range of 0.01–0.05 mM.^[19–20]

Among the three metal salts studied, *C. necator* H16 exhibited the highest susceptibility to CoCl_2 (Figure S1). At concentrations of 8 and 10 μM of CoCl_2 , a significant reduction in growth was observed, with concentrations exceeding 10 μM proving to be severely detrimental to growth. In contrast, *C. necator* H16 demonstrated a higher tolerance for MnCl_2 , as concentrations up to 10 mM had no significant impact on microbial growth. Even at concentrations as high as 15 and 25 mM, growth was observed, albeit at a slower rate. Addition of 0.6–0.8 mM ZnCl_2 led to a reduced growth, with minimal growth observed beyond this concentration range. Based on the growth data, the concentrations of 10 μM CoCl_2 , 15 mM MnCl_2 , and 0.7 mM ZnCl_2 were selected to establish an aALE workflow. At these specific concentrations, microbial growth was feasible, although at a reduced rate, potentially indicating a decrease in DNA synthesis and/or the introduction of errors during DNA replication. The latter effect was sought to increase genetic diversity.

To assess the broader applicability of divalent metal cation-mediated genetic diversity creation, we also examined the effect of MnCl_2 on the microbial growth of *E. coli*, the prevalent chassis in synthetic biology and biomanufacturing. Consistently, we observed growth retardation with increasing MnCl_2 concentration (Figure S2).

3.2 | Divalent metal ions altered the growth performance of microbial populations in 10% v/v glycerol

To expedite the process of ALE, we adopted a scheme commonly employed for protein evolution, which involves creating genetic diversity followed by selecting improved variants. In our aALE workflow (Figure 1), cells were initially subjected to random mutagenesis

through cultivation in the presence of 10 μM CoCl_2 , 15 mM MnCl_2 , or 0.7 mM ZnCl_2 . Subsequently, the cells were cultivated under selective conditions to enrich the population displaying the desired phenotype.

In order to showcase the practical application of the aALE method, we opted to adapt *C. necator* H16 to utilize 10% v/v glycerol. This particular adaptation was guided by two key considerations. Firstly, glycerol stands as an appealing feedstock for biomanufacturing purposes.^[21–22] Secondly, while ALE has been applied to enhance glycerol utilization in various microbes, it has typically been carried out at lower glycerol concentrations. For example, adaptation of *C. necator* H16 was conducted at 0.5% v/v glycerol,^[4] *E. coli* at 0.2% v/v,^[23] and *S. cerevisiae* at 1% v/v.^[24] The adaptation to 10% v/v glycerol is challenging, likely due to the cellular dehydration experienced, which adversely affects cell viability.^[25]

Through the application of aALE, we successfully generated *C. necator* H16 microbial populations that exhibited a higher growth rate and reached higher final OD_{650} values in the presence of 10% v/v glycerol (as indicated by the arrows in Figure 2). This effect was noticeable after three cycles of evolution when cells were exposed to 10 μM CoCl_2 , with each cycle defined as a sequence of mutagenesis followed by selection. When cells were treated with 15 mM MnCl_2 and 0.7 mM ZnCl_2 , this enhanced growth was observed after only two cycles of evolution. Continued iterations revealed an opposing trend, characterized by slower growth and lower final OD_{650} values, which suggested the overaccumulation of detrimental mutations.

Furthermore, we conducted the cultivation of *C. necator* H16 in 10% v/v glycerol without any prior treatment involving divalent metal cations (Figure 2D). It is interesting to note that *C. necator* H16 demonstrated the capacity to grow at this concentration. Despite conducting six rounds of serial cultivations, no discernible improvement in growth rate or final OD_{650} value was observed. This implies that achieving an improved performing population would require an extended duration if we were to continue with successive cultivation in 10% v/v glycerol. Leveraging the amplification of genetic diversity facilitated by the use of divalent metal cations, we captured rare beneficial mutations, effectively shortening the time required for enhancement.

3.3 | Adapted variants grew better at 10% v/v and 15% v/v glycerol

Populations from the second cycle (MnCl_2 - or ZnCl_2 -treated cells) and the third cycle (CoCl_2 -treated cells) were spread on an agar plate, with subsequent individual positive clones subjected to further confirmation and detailed characterization.

In Figure S3, we compared the growth performance of *C. necator* H16 variants (Mn-C2-B11 and Mn-C2-F11), isolated from the population that underwent two cycles of 15 mM MnCl_2 treatment, against the wild type (WT) and v6C6 variant obtained from a prior ALE study.^[4] The v6C6 variant was isolated after six rounds of sequential cultivation at 0.5% v/v glycerol. As part of this comparison, we included a variant (Mn-C1-D3) isolated from the population that underwent only one cycle of 15 mM MnCl_2 treatment, aiming to assess whether a single

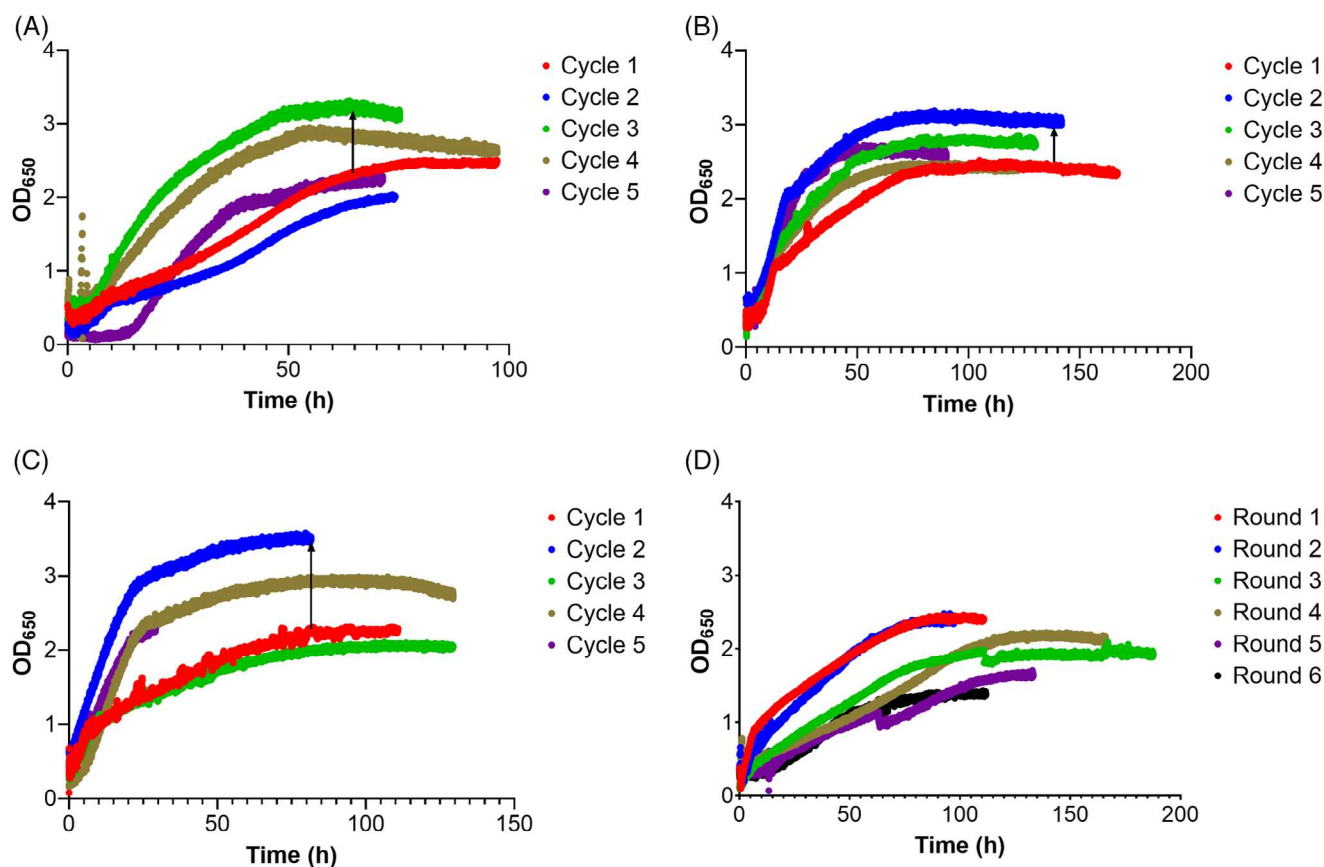


FIGURE 2 The growth of *C. necator* H16 in 10% v/v glycerol in Chi.Bio, following treatment with 10 μM CoCl_2 (A), 15 mM MnCl_2 (B), 0.7 mM ZnCl_2 (C), and in the absence of treatment (D). The black arrows signify an increase in the final OD_{650} values.

aALE cycle sufficed to isolate improved variants. Growth comparisons were conducted in 96-well microplate using two carbon sources: 1% w/v sodium gluconate, a preferred carbon source of *C. necator* H16,^[26] and 5% v/v glycerol. All variants exhibited similar growth in gluconate. However, at 5% v/v glycerol, all ALE-derived variants demonstrated superior growth compared to the WT. The v6C6 variant outperformed all other variants at this particular glycerol concentration. Remarkably, the performance of the Mn-C1-D3 variant was found to be on par with that of v6C6, underscoring the advantage of aALE in expediting the process of identifying improved variants. Furthermore, we characterized the variants derived from populations treated with CoCl_2 and ZnCl_2 and noted similar trends (Figure S4).

Subsequently, we conducted a comprehensive growth comparison involving variant Mn-C2-B11 alongside the WT, v6C6, Co-C3-F3, and Zn-C2-G5, at a larger cultivation scale of 20 mL in three distinct glycerol concentrations [5% v/v, 10% v/v, and 15% v/v], employing a personal bioreactor RTS-1. Variants Co-C3-F3 and Zn-C2-G5 were isolated from populations that underwent three cycles of 10 μM CoCl_2 treatment and two cycles of 0.7 mM ZnCl_2 treatment, respectively. All the microbial growth curves obtained from the personal bioreactor RTS-1 were fitted using the Gompertz model in GraphPad Prism (Table S1).

At 5% v/v glycerol, the results were consistent with the findings obtained earlier using the 96-well microplate. v6C6 remained the

most proficient variant at this concentration, closely trailed by Mn-C2-B11 (Figure S5A). However, at 10% v/v glycerol, the concentration at which aALE was conducted, Mn-C2-B11 exhibited the best growth (Figure 3A). Additionally, we conducted a comparative growth at 15% v/v, a significantly higher concentration than the aALE condition of 10% v/v. The results demonstrated a consistent trend, with Mn-C2-B11 emerging as the superior performer at this concentration (Figure S5C). The disparities observed between the 5% v/v and higher concentrations [10% v/v or 15% v/v] potentially underscored the superior ability of variants obtained at 10% v/v to withstand high osmotic stress, in addition to displaying improved glycerol utilization.

To address potential biases in spectrophotometric measurements caused by factors such as cell morphology and biomaterials produced by the cells (e.g., PHA), we complemented our real-time growth study in the personal bioreactor RTS-1 with additional measurements. We determined the OD_{600} values of the final cultures, measured the dry cell weights, and quantified the glycerol concentration in the spent medium using HPLC (Table S2 and Figure S6). A strong correlation was observed between dry cell weight and OD_{600} measurements (Pearson correlation coefficient of 0.8711, with p (two-tailed) < 0.0001) (Figure S7). The glycerol consumption data were consistent with the spectrophotometric measurements. Specifically, v6C6 consumed more glycerol at 5% v/v glycerol, whereas Mn-C2-B11 consumed more glycerol at higher glycerol concentrations of 10% v/v (Figure 3B) and 15%

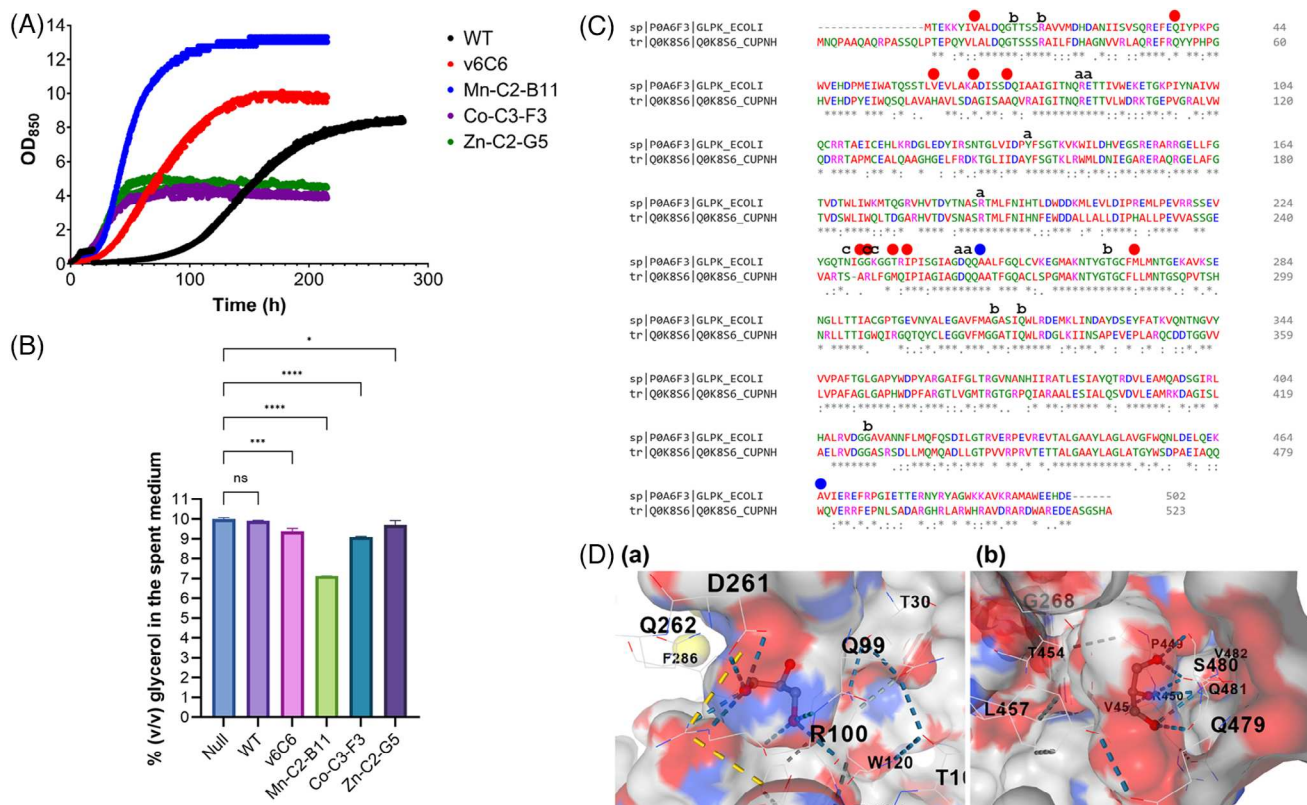


FIGURE 3 (A) The growth of variants Mn-C2-B11 (blue), Co-C3-F3 (purple), and Zn-C2-G5 (green), in comparison to the wild type (WT) (black) and v6C6 (red), in 10% v/v glycerol. WT refers to *C. necator* H16 WT, the strain prior to being subjected to adaptive laboratory evolution (ALE). The cultivations were carried out in a personal bioreactor RTS-1. (B) At the end of the cultivation, the remaining glycerol in the spent medium was quantified using high-performance liquid chromatography (HPLC). Statistical analysis was conducted using one-way analysis of variance (ANOVA) in GraphPad Prism. (C) Protein sequence alignment between the glycerol kinase from *E. coli* (UniProt P0A6F3) and that from *C. necator* H16 (Q0K8S6) is illustrated. The alignment was performed using Clustal Omega.^[27] Mutations discovered in glycerol-adapted *E. coli* and *C. necator* H16 through ALE are depicted with red dots and blue dots, respectively. Amino acids situated within the active site of the glycerol kinase are denoted using small letters, where “a” indicates interaction with glycerol, “b” denotes interaction with ADP, and “c” represents interaction with a phosphate ion.^[28] (D) The primary glycerol binding site (a) was identified in GlpK WT, single mutant (W480S), and double mutant (A264V, W480S). An additional glycerol binding site (b) was found in both the single and double mutants, where the S480 side chain interacts with one of the hydroxyl groups of glycerol.

v/v. Furthermore, for these two efficient glycerol users (Mn-C2-B11 and v6C6), there was also a strong correlation between dry cell weight and glycerol consumption (Pearson correlation coefficient of 0.8813, with p (two-tailed) = 0.0203) (Figure S7).

3.4 | SNVs and InDels were detected in all aALE variants

The genomes of the WT, Mn-C2-B11, Co-C3-F3, and Zn-C2-G5 were sequenced and subsequently compared against the reference genomes (GenBank accession numbers CP039287, CP039288, and CP039289).^[29] SNVs (Table S3) and insertions/deletions (InDels) (Table S4) were detected in all variants originating from aALE. These mutations are primarily located in chromosome 1. MnCl₂ and CoCl₂ exhibited significantly higher mutagenic effects compared to ZnCl₂ (Table S5), in line with the findings previously documented by Loeb and coworkers.^[17,18]

Typically transition-heavy mutations are generated in epPCR.^[8,9] In our aALE-derived variants, we identified both transition and transversion mutations. Moreover, the observed mutation count was higher in comparison to the variants obtained through serial cultivation, such as v6C6.^[4]

The dataset from the small number of genome sequences was limited and insufficient to draw a broad conclusion. Nevertheless, our sequencing results confirmed two significant aspects: the induction of mutations by divalent metal cations and their effective application in expanding genetic diversity.

3.5 | Variant Mn-C2-B11 carries two nonsynonymous mutations in the gene encoding glycerol kinase

Variant Mn-C2-B11, displaying the most robust growth at 10% v/v and 15% v/v glycerol (Figure 3A and Figure S5), carries two

nonsynonymous mutations in the *glpK* gene, resulting in A264V and W480S substitutions within the glycerol kinase (GlpK) sequence. The occurrence of two mutations within a single protein-coding gene is statistically uncommon and underscores the impact of treating cells with 15 mM MnCl₂, effectively inducing a high mutation rate that aligns precisely with our intended outcomes within the aALE workflow. GlpK plays a crucial role in the initial step of glycerol metabolism, facilitating the conversion of triol into glycerol-3-phosphate. Moreover, the W480S substitution in GlpK was also observed in the Co-C3-F3 variant within this study and the v6C6 variant from a previous ALE study.^[4] Additionally, mutations in the *glpK* gene were also highly recurrent in a glycerol-adapted *E. coli*^[23,30–33] (Table S6), emphasizing the significance of GlpK in glycerol assimilation.

While the functional consequence of the W480S substitution remains unclear, it is worth noting that residue A264 is positioned within the active site of GlpK, adjacent to D261 and Q262, which are highly conserved among glycerol kinase sequences and play a role in interacting with glycerol^[28] (Figure 3C).

ColabFold^[34] was utilized to predict the 3-D structures of GlpK WT, a single mutant (SM) with a W480S substitution in the v6C6 variant isolated in the previous ALE study,^[4] and a double mutant (DM) with both A264V and W480S substitutions in the Mn-C2-B11 variant identified in the current aALE study. As shown in Figure S8, the predicted structures exhibit high similarity, with low RMSD values in all pairwise comparisons: 0.257 Å for the WT-SM pair, 0.416 Å for the WT-DM pair, and 0.556 Å for the SM-DM pair.

Using the predicted structures, we conducted cavity-detection guided blind docking with a glycerol molecule using CD-Dock 2.^[35] In the WT structure, a large cavity (4914 Å³) was identified as the primary glycerol binding site (Figure 3D), with a low Vina score of –4.2 (Table S7). This cavity aligns with the experimentally determined active site of *E. coli*, where glycerol interacts with highly conserved residues including R100, E101, Y152, D261, and Q262. Interestingly, in both the SM and DM structures, this cavity is significantly smaller (1027 Å³ in SM and 1147 Å³ in DM). Additionally, a new glycerol binding site with a favorable Vina score was discovered, where glycerol interacts with the side chain of S480 (Figure 3D). The reduction in cavity size of the main glycerol binding site might enhance catalysis by restricting nonproductive random movement. Furthermore, the presence of an additional glycerol binding site could increase local glycerol concentration, thereby favoring catalysis.

A comprehensive biochemical characterization of GlpK variants would be essential to gain a thorough understanding of the functional implications of these mutations. However, this analysis falls outside the scope of this article, which centers on the aALE workflow.

3.6 | Potential augmented stress tolerance in aALE variants

Variants Mn-C2-B11 and Co-C3-F3 also carry a G253W substitution in the YgcG family protein, a protein that is predicted to have a transmembrane domain and is considered a putative phosphatase.

This substitution was absent in variant Zn-C2-G5 and the WT, which served as the starting point for our aALE (Table S3). Examination using STRING^[36] indicated that YgcG is functionally associated with the membrane stress resistance protein YqcG in *E. coli* (Figure S9). Intriguingly, the same protein was mutated at the identical position in a recent ALE study, where *C. necator* H16 underwent evolution for enhanced halotolerance.^[5] Commencing from a W253 genotype, the identified halotolerant variant carried a W253G mutation, thereby reversing W253 back to G253.

Residue G253 is situated in the glycine-rich C-terminal region of YgcG. Glycine-rich proteins are known to play roles in cellular stress responses and signaling.^[37] The 3-D structures of YgcG WT and the G253W mutant, predicted using ColabFold, showed high similarity with an RMSD of 0.38 Å (Figure S10). Since the mutation is located in the largely disordered C-terminal region, it is challenging to determine if the mutation causes a different orientation of the C-terminal region relative to the structured N-terminal region.

4 | CONCLUSIONS

In conclusion, we have successfully devised an accelerated and cost-effective ALE workflow, demonstrating its effectiveness in evolving *C. necator* H16 for enhanced tolerance toward high glycerol concentrations. This method offers several advantages. Firstly, by amplifying genetic diversity, we significantly reduce the time required to attain a desired phenotype. In this study, we were able to identify an improved variant after just one cycle of aALE, underscoring the efficiency of this approach. By way of comparison, a previous study on ALE of *E. coli* MG1655 in M9 minimal medium supplemented with 0.2% glycerol showed that growth rates could be increased by more than two-fold through log-phase serial transfers spanning over 800 generations.^[33] In another related work, *E. coli* W strain underwent adaptive evolution over 1300 generations.^[23] Secondly, our aALE workflow does not necessitate a genetically modified strain (e.g., the use of a *mutS* knock-out derivative^[33]) to initiate an ALE, nor does it rely on specialized genetic tools (e.g., Tn5 mutagenesis^[38]). Thirdly, our method does not depend on DNA-modifying agents, which are frequently categorized as carcinogens. Lastly, this methodology can be readily adapted to other microbial strains, enhancing its versatility and applicability.

AUTHOR CONTRIBUTIONS

Sepwin Nosten Sitompul: Data curation, formal analysis, investigation, validation, visualization, writing – original draft; Laura Andrea Diaz Garcia: Data curation, formal analysis; Joseph Price: writing – review & editing; Kang Lan Tee: conceptualization, data curation, formal analysis, funding acquisition, investigation, methodology, project administration, resources, supervision, writing – review & editing; Tuck Seng Wong: conceptualization, data curation, formal analysis, funding acquisition, investigation, methodology, project administration, resources, supervision, visualization, writing – original draft, writing – review & editing.

ACKNOWLEDGMENTS

The authors express their sincere gratitude to the following organizations for their financial support: the UKRI Global Challenges Research Fellowship (to K.L.T.), EPSRC New Investigator Award (EP/X025853/1, to K.L.T.), the RAEng | Leverhulme Trust Senior Research Fellowship (LTSRF1819-15-21, to T.S.W.), the National Research Council of Thailand (P2250317/3, to T.S.W.), the Directorate General of Higher Education, Research, and Technology, Ministry of Education, Culture, Research, and Technology of the Republic of Indonesia (PhD scholarship to S.N.S.) and the Department of Chemical & Biological Engineering (PhD studentship to L.A.D.G.).

CONFLICT OF INTEREST STATEMENT

The authors declare no commercial or financial conflicts of interest.

DATA AVAILABILITY STATEMENT

The data that supports the findings of this study is available in the supplementary material of this article.

ORCID

Kang Lan Tee  <https://orcid.org/0000-0001-9458-733X>

Tuck Seng Wong  <https://orcid.org/0000-0001-7689-9057>

REFERENCES

- Mavrommati, M., Daskalaki, A., Papanikolaou, S., & Aggelis, G. (2022). Adaptive laboratory evolution principles and applications in industrial biotechnology. *Biotechnology Advances*, 54, 107795. <https://doi.org/10.1016/j.biotechadv.2021.107795>
- Sandberg, T. E., Salazar, M. J., Weng, L. L., Palsson, B. O., & Feist, A. M. (2019). The emergence of adaptive laboratory evolution as an efficient tool for biological discovery and industrial biotechnology. *Metabolic Engineering*, 56, 1. <https://doi.org/10.1016/j.ymben.2019.08.004>
- Wang, G., Li, Q., Zhang, Z., Yin, X., Wang, B., & Yang, X. (2023). Recent progress in adaptive laboratory evolution of industrial microorganisms. *Journal of Industrial Microbiology & Biotechnology*, 50, kuac023. <https://doi.org/10.1093/jimb/kuac023>
- Gonzalez-Villanueva, M., Galaiya, H., Staniland, P., Staniland, J., Savill, I., Wong, T. S., & Tee, K. L. (2019). Adaptive laboratory evolution of *Cupriavidus necator* H16 for carbon co-utilization with glycerol. *International Journal of Molecular Sciences*, 20, 5737. <https://doi.org/10.3390/ijms20225737>
- Adams, J. D., Sander, K. B., Criddle, C. S., Arkin, A. P., & Clark, D. S. (2023). Engineering osmolyte susceptibility in *Cupriavidus necator* and *Escherichia coli* for recovery of intracellular products. *Microbial Cell Factories*, 22, 69. <https://doi.org/10.1186/s12934-023-02064-8>
- Calvey, C. H., Sanchez, I. N. V., White, A. M., Kneucker, C. M., Woodworth, S. P., Alt, H. M., Eckert, C. A., & Johnson, C. W. (2023). Improving growth of *Cupriavidus necator* H16 on formate using adaptive laboratory evolution-informed engineering. *Metabolic Engineering*, 75, 78. <https://doi.org/10.1016/j.ymben.2022.10.016>
- Wickham-Smith, C., Malys, N., & Winzer, K. (2023). Improving carbon monoxide tolerance of *Cupriavidus necator* H16 through adaptive laboratory evolution. *Frontiers in Bioengineering and Biotechnology*, 11, 1178536. <https://doi.org/10.3389/fbioe.2023.1178536>
- Tee, K. L., & Wong, T. S. (2013). Polishing the craft of genetic diversity creation in directed evolution. *Biotechnology Advances*, 31, 1707. <https://doi.org/10.1016/j.biotechadv.2013.08.021>
- Wong, T. S., Zhurina, D., & Schwaneberg, U. (2006). The diversity challenge in directed protein evolution. *Combinatorial Chemistry & High Throughput Screening*, 9, 271. <https://doi.org/10.2174/138620706776843192>
- Schlegel, H. G., Gottschalk, G., & Von Bartha, R. (1961). Formation and utilization of poly- β -hydroxybutyric acid by Knallgas bacteria (*Hydrogenomonas*). *Nature*, 191, 463. <https://doi.org/10.1038/191463a0>
- Steel, H., Habgood, R., Kelly, C. L., & Papachristodoulou, A. (2020). In situ characterisation and manipulation of biological systems with Chi.Bio. *PLoS Biology*, 18, e3000794. <https://doi.org/10.1371/journal.pbio.3000794>
- Cock, P. J., Fields, C. J., Goto, N., Heuer, M. L., & Rice, P. M. (2010). The Sanger FASTQ file format for sequences with quality scores, and the Solexa/Illumina FASTQ variants. *Nucleic Acids Research*, 38, 1767. <https://doi.org/10.1093/nar/gkp1137>
- DePristo, M. A., Banks, E., Poplin, R., Garimella, K. V., Maguire, J. R., Hartl, C., Philippakis, A. A., del Angel, G., Rivas, M. A., Hanna, M., McKenna, A., Fennell, T. J., Kernysky, A. M., Sivachenko, A. Y., Cibulskis, K., Gabriel, S. B., Altshuler, D., & Daly, M. J. (2011). A framework for variation discovery and genotyping using next-generation DNA sequencing data. *Nature Genetics*, 43, 491. <https://doi.org/10.1038/ng.806>
- Wang, K., Li, M., & Hakonarson, H. (2010). ANNOVAR: Functional annotation of genetic variants from high-throughput sequencing data. *Nucleic Acids Research*, 38, e164. <https://doi.org/10.1093/nar/gkq603>
- Chandrangsu, P., Rensing, C., & Helmann, J. D. (2017). Metal homeostasis and resistance in bacteria. *Nature Reviews Microbiology*, 15, 338. <https://doi.org/10.1038/nrmicro.2017.15>
- Foster, A. W., Young, T. R., Chivers, P. T., & Robinson, N. J. (2022). Protein metalation in biology. *Current Opinion in Chemical Biology*, 66, 102095. <https://doi.org/10.1016/j.cbpa.2021.102095>
- Sirover, M. A., & Loeb, L. A. (1976). Infidelity of DNA synthesis *in vitro*: Screening for potential metal mutagens or carcinogens. *Science*, 194, 1434. <https://doi.org/10.1126/science.1006310>
- Zakour, R. A., Kunkel, T. A., & Loeb, L. A. (1981). Metal-induced infidelity of DNA synthesis. *Environmental Health Perspectives*, 40, 197. <https://doi.org/10.1289/ehp.8140197>
- Alessa, A. H. A., Tee, K. L., Gonzalez-Perez, D., Omar Ali, H. E. M., Evans, C. A., Trevaskis, A., Xu, J. H., & Wong, T. S. (2019). Accelerated directed evolution of dye-decolorizing peroxidase using a bacterial extracellular protein secretion system (BENNY). *Bioresources and Bioprocessing*, 6, 20. <https://doi.org/10.1186/s40643-019-0255-7>
- Jajesniak, P., Tee, K. L., & Wong, T. S. (2019). PTO-QuickStep: A fast and efficient method for cloning random mutagenesis libraries. *International Journal of Molecular Sciences*, 20, 3908. <https://doi.org/10.3390/ijms20163908>
- Keita, V. M., Gonzalez-Villanueva, M., Wong, T. S., & Tee, K. L. (2020). In V. Singh, A. K. Singh, P. Bhargava, M. Joshi, & C. G. Joshi (Eds.), *Engineering of microbial biosynthetic pathways* (p. 245). Springer Singapore. https://doi.org/10.1007/978-981-15-2604-6_16
- Keita, V. M., Lee, Y. Q., Lakshmanan, M., Ow, D. S.-W., Staniland, P., Staniland, J., Savill, I., Tee, K. L., Wong, T. S., & Lee, D.-Y. (2024). Evaluating oleaginous yeasts for enhanced microbial lipid production using sweetwater as a sustainable feedstock. *Microbial Cell Factories*, 23, 63. <https://doi.org/10.1186/s12934-024-02336-x>
- Kim, K., Hou, C. Y., Choe, D., Kang, M., Cho, S., Sung, B. H., Lee, D. H., Lee, S. G., Kang, T. J., & Cho, B. K. (2022). Adaptive laboratory evolution of *Escherichia coli* W enhances gamma-aminobutyric acid production using glycerol as the carbon source. *Metabolic Engineering*, 69, 59. <https://doi.org/10.1016/j.ymben.2021.11.004>
- Kawai, K., Kanesaki, Y., Yoshikawa, H., & Hirasawa, T. (2019). Identification of metabolic engineering targets for improving glycerol assimilation ability of *Saccharomyces cerevisiae* based on adaptive laboratory evolution and transcriptome analysis. *Journal of Bioscience and Bioengineering*, 128, 162. <https://doi.org/10.1016/j.jbiosc.2019.02.001>

25. Mille, Y., Beney, L., & Gervais, P. (2005). Compared tolerance to osmotic stress in various microorganisms: Towards a survival prediction test. *Biotechnology and Bioengineering*, 92, 479. <https://doi.org/10.1002/bit.20631>
26. Volodina, E., Raberg, M., & Steinbuchel, A. (2016). Engineering the heterotrophic carbon sources utilization range of *Ralstonia eutropha* H16 for applications in biotechnology. *Critical Reviews in Biotechnology*, 36, 978. <https://doi.org/10.3109/07388551.2015.1079698>
27. Sievers, F., Wilm, A., Dineen, D., Gibson, T. J., Karplus, K., Li, W., Lopez, R., McWilliam, H., Remmert, M., Soding, J., Thompson, J. D., & Higgins, D. G. (2011). Fast, scalable generation of high-quality protein multiple sequence alignments using Clustal Omega. *Molecular Systems Biology*, 7, 539. <https://doi.org/10.1038/msb.2011.75>
28. Rani, R. M., Syngkli, S., Nongkhlaw, J., & Das, B. (2023). Expression and characterisation of human glycerol kinase: The role of solubilising agents and molecular chaperones. *Bioscience Reports*, 43, BSR20222258. <https://doi.org/10.1042/BSR20222258>
29. Little, G. T., Ehsaan, M., Arenas-Lopez, C., Jawed, K., Winzer, K., Kovacs, K., & Minton, N. P. (2019). Complete genome sequence of *Cupriavidus necator* H16 (DSM 428). *Microbiology Resource Announcements*, 8, e00814–e00819. <https://doi.org/10.1128/MRA.00814-19>
30. Cheng, K. K., Lee, B. S., Masuda, T., Ito, T., Ikeda, K., Hirayama, A., Deng, L., Dong, J., Shimizu, K., Soga, T., Tomita, M., Palsson, B. O., & Robert, M. (2014). Global metabolic network reorganization by adaptive mutations allows fast growth of *Escherichia coli* on glycerol. *Nature Communications*, 5, 3233. <https://doi.org/10.1038/ncomms4233>
31. Fong, S. S., Joyce, A. R., & Palsson, B. O. (2005). Parallel adaptive evolution cultures of *Escherichia coli* lead to convergent growth phenotypes with different gene expression states. *Genome Research*, 15, 1365. <https://doi.org/10.1101/gr.3832305>
32. Herring, C. D., Raghunathan, A., Honisch, C., Patel, T., Applebee, M. K., Joyce, A. R., Albert, T. J., Blattner, F. R., van den Boom, D., Cantor, C. R., & Palsson, B. O. (2006). Comparative genome sequencing of *Escherichia coli* allows observation of bacterial evolution on a laboratory timescale. *Nature Genetics*, 38, 1406. <https://doi.org/10.1038/ng1906>
33. Kang, M., Kim, K., Choe, D., Cho, S., Kim, S. C., Palsson, B., & Cho, B. K. (2019). Inactivation of a mismatch-repair system diversifies genotypic landscape of *Escherichia coli* during adaptive laboratory evolution. *Frontiers in Microbiology*, 10, 1845. <https://doi.org/10.3389/fmicb.2019.01845>
34. Mirdita, M., Schütze, K., Moriwaki, Y., Heo, L., Ovchinnikov, S., & Steinegger, M. (2022). ColabFold: Making protein folding accessible to all. *Nature Methods*, 19, 679. <https://doi.org/10.1038/s41592-022-01488-1>
35. Liu, Y., Yang, X., Gan, J., Chen, S., Xiao, Z. X., & Cao, Y. (2022). CB-Dock2: Improved protein–ligand blind docking by integrating cavity detection, docking and homologous template fitting. *Nucleic Acids Research*, 50, W159. <https://doi.org/10.1093/nar/gkac394>
36. von Mering, C., Jensen, L. J., Snel, B., Hooper, S. D., Krupp, M., Foglierini, M., Jouffre, N., Huynen, M. A., & Bork, P. (2005). STRING: Known and predicted protein-protein associations, integrated and transferred across organisms. *Nucleic Acids Research*, 33, D433. <https://doi.org/10.1093/nar/gki005>
37. Czolpinska, M., & Rurek, M. (2018). Plant glycine-rich proteins in stress response: An emerging, still prospective story. *Frontiers in Plant Science*, 9, 302. <https://doi.org/10.3389/fpls.2018.00302>
38. Strittmatter, C. S., Eggers, J., Biesgen, V., Pauels, I., Becker, F., & Steinbuchel, A. (2022). The reliance of glycerol utilization by *Cupriavidus necator* on CO₂ fixation and improved glycerol catabolism. *Applied Microbiology and Biotechnology*, 106, 2541. <https://doi.org/10.1007/s00253-022-11842-0>

SUPPORTING INFORMATION

Additional supporting information can be found online in the Supporting Information section at the end of this article.

How to cite this article: Sitompul, S. N., Diaz Garcia, L. A., Price, J., Tee, K. L., & Wong, T. S. (2024). Fast-track adaptive laboratory evolution of *Cupriavidus necator* H16 with divalent metal cations. *Biotechnology Journal*, 19, e2300577. <https://doi.org/10.1002/biot.202300577>